Scanning Electrochemical Microscopy. 51. Studies of Self-Assembled Monolayers of DNA in the Absence and Presence of Metal Ions

Biao Liu and Allen J. Bard*

Department of Chemistry and Biochemistry, The University of Texas at Austin, Austin, Texas 78712

Chen-Zhong Li and Heinz-Bernhard Kraatz

Department of Chemistry, University of Saskatchewan, 110 Science Place, Saskatoon, SK S7N 5C9, Canada

Received: October 29, 2004; In Final Form: January 14, 2005

Scanning electrochemical microscopy was used to examine electron transfer across a self-assembled monolayer of thiol-modified DNA duplexes on a gold electrode. The apparent rate constant for heterogeneous ET from a solution redox probe, $Fe(CN)_6^{3-/4-}$, to the gold surface through ds-DNA was 4.6 ($\pm$0.2) $\times$ 10^{-7} cm/s. With the addition of Zn^{2+}, which resulted in the formation of a metalated DNA (M-DNA) monolayer, the rate constant increased to 5.0 ($\pm$0.3) $\times$ 10^{-6} cm/s. Upon treating M-DNA with EDTA, the zinc ions were released from the monolayer and the original rate constant for the DNA duplexes was restored. The enhanced ET rate was also observed at a DNA monolayer treated with Ca^{2+} or Mg^{2+}, which does not complex by the DNA bases to form M-DNA. The binding of these cations facilitated the monolayer penetration by the probe mediator $Fe(CN)_6^{3-/4-}$ and accordingly caused an increased redox signal of the mediator at the ds-DNA-modified electrode. Cationic or neutral mediators were not blocked by the ds-DNA monolayer. These results suggest that although the increased electron transport through M-DNA could partially be ascribed to the intrinsic enhancement of electric conductivity of M-DNA, which has been confirmed by photochemical studies, the change in the surface charge of DNA monolayers on the electrode caused by the binding of metal ions to DNA molecules may play a more important role in the enhancement of current with M-DNA.

Introduction

The transport of charges (electrons and holes) through DNA has been the subject of numerous studies, with DNA being variously described as an insulator, semiconductor, or molecular wire. Mechanistic studies have addressed charge transport in double-stranded DNA and have provided evidence for combinations of tunneling and hopping, (e.g., hole transfer) involving the π-stacked bases on the interior of the duplex. The prevailing picture now seems to be that charge transport involves hopping, for example, among G-centers, and that the base sequence plays an important role in the process.[1−5] The self-assembly of DNA has also attracted significant attention, for example, with the use of DNA as a template for the construction of electronic nanocircuits. In addition, layers of DNA have been proposed as the basis of electrochemical devices that can recognize DNA hybridization and, through this, identify target DNA strands. However, before such construction can be undertaken, the electronic properties of DNA need to be explored in detail.

Lee and co-workers reported a new form of DNA, called M-DNA, in which divalent metal ions are associated with individual bases in the DNA duplex.[6] In such structures, the metal ion was reported to replace one of the protons on the hydrogen-bonded interface of the two interacting bases. Titration experiments have shown that addition of Zn^{2+} causes the loss of specific proton signals associated with the hydrogen-bonding between bases on the two complementary strands.[6] M-DNA forms under mildly basic conditions in the presence of divalent metal ions such as Zn^{2+} (pH 8.5) and at low ionic strength. Other metals such as Ni^{2+} and Co^{2+} also form M-DNA, whereas Ca^{2+} and Mg^{2+} are said only to associate with the phosphate backbone. M-DNA and B-DNA are readily interconvertable, so that the self-assembly and molecular recognition properties are not lost.[7] Several experimental results suggested that M-DNA has electronic properties that differ significantly from those of B-DNA.[7,8] Electron transfer (ET) in M-DNA was reported to occur, even over 500 base pairs or approximately 170 nm, following an electron "hopping" mechanism.[9] Recent electrochemical, for example, cyclic voltammetry (CV), studies of self-assembled monolayers (SAMs) of ds-DNA and M-DNA on gold surfaces have indicated that upon conversion of B-DNA to M-DNA the rate of ET through DNA monolayers increased.[10,11]

We have previously used scanning electrochemical microscopy (SECM) to study charge transfer through SAMs of alkanethiols.[12] SECM has a number of advantages over transient electrochemical methods such as CV. The small tip size means that only a small area of a SAM is addressed, making the measured response less susceptible to effects from pinholes and defects in the film. The small tip currents, usually in the nA range, make the technique immune to uncompensated resistance effects, which is important in quantitative kinetic studies. Moreover, because the measurements involve steady-state currents, double-layer capacitive effects and the electrochemical response of adsorbed species are unimportant in the measurements. Thus, we thought it useful to repeat ET studies with a double-stranded DNA (ds-DNA)-modified electrode by SECM, including effects of conversion to M-DNA. We have measured the apparent rate of electron-transfer between a substrate gold

* Corresponding author. E-mail: ajbard@mail.utexas.edu.

10.1021/jp045050v CCC: $30.25
Published on Web 03/01/2005

electrode through a ds-DNA molecular bridge attached to the electrode surface with a disulfide linker, and the frequently used mediator, $Fe(CN)_6^{3-/4-}$, as well as other redox mediators, in solution by SECM. While the apparent ET rates measured with SECM were qualitatively in agreement with those previously obtained from voltammetric measurements for $Fe(CN)_6^{3-/4-}$, the overall results suggest that penetration of the DNA layers by the mediator plays an important role in the observed electrochemical response.

Experimental Section

Chemicals. $Ru(NH_3)_6Cl_3$ and acetylferrocene were purchased from Strem Chemicals (Newburyport, MA). Potassium ferricyanide was obtained from MCB Manufacturing Chemicals Inc. (Cincinnati, OH), EDTA from EM Science (Gibbstown, NJ), and ferrocenecarboxaldehyde, ferrocenemethanol, and $ZnClO_4$ from Aldrich (Milwaukee, WI). All commercial chemicals were used as received. Tris(2,2′-bipyridyl)cobalt(II) dichloride $[Co(bpy)_3Cl_2]$ and tris(1,10-phenanthroline)cobalt(II) dichloride $[Co(phen)_3Cl_2]$ were prepared according to previously reported procedures.[2,6] All other chemicals used for preparing supporting electrolytes (NaCl, $NaClO_4$, $HClO_4$, Tris, $CaAc_2$, $MgAc_2$) were reagent grade. Solutions were prepared in high-purity water ($\rho = 18$ MΩ cm) from a Millipore Milli-Q water purification system.

DNA Synthesis. Oligonucleotides were synthesized using standard solid-phase phosphoramidite chemistry on CPG (controlled pore glass).[13] The synthesis was carried out on a fully automated Beckman 1000M DNA Synthesizer at the Plant Biotechnology Institute (PBI-NRC, Saskatoon, Canada). After termination of the synthesis, concentrated ammonia was used to remove the DNA from the CPG. The 5′-terminal amine group in the deprotected oligonucleotide was further derivatized with dithiothreitol (Glen Research, Sterling, VA) to produce 5′-dithiol-terminated oligonucleotides.[14] The oligonucleotides were purified by two-step reversed-phase HPLC with a C18 column, using acetonitrile/triethylamine acetate (TEAA) (pH 7.4). Finally, the synthesized oligonucleotides were characterized by matrix-assisted laser desorption ionization time-of-flight mass spectroscopy (MALDI-TOFMS). Calculated molecular ions were identical to those obtained experimentally. The 20-base sequences of the disulfide-modified oligonucleotide and its complementary strand are the following:

SS-5′-GTCACGATGGCCCAGTAGTT-3′ **1**

5′-AACTACTGGGCCATCGTGAC-3′ **2**

where SS represents the dithiol group that can attach to the Au substrate.

DNA Monolayer Deposition. 1 was hybridized with **2** by combining equimolar amounts of each strand (in 20 mM tris-ClO_4, pH 8.6) for a final solution of 0.2 mM duplex. The mixture was heated at 50 °C for 5 min and then kept at room-temperature overnight. Just before deposition on the gold surfaces, 0.4 M $NaClO_4$ was added to the DNA incubation solution. The gold substrates were prepared by thermal evaporation of chromium followed by gold (99.99% purity) onto a glass slide at approximately 1×10^{-6} Torr. The thickness of the chromium and gold films were typically 30 and 1500−2000 Å, respectively. Before modification, the gold surfaces were cleaned through sequential and repetitive immersion in sulfochromic acid (saturated $Na_2Cr_2O_7$ in concentrated H_2SO_4) and 5% HF,[15] and then thoroughly rinsed with Milli-Q water and dried in a stream of pure argon. A volume of 50 μL of ds-DNA solution (0.2 mM) was added onto the cleaned gold electrode, which was then kept in a small Petri dish (35×10 mm). The small Petri dish was wrapped with Parafilm in a larger closed Petri dish (100×15 mm) containing several drops of water, to maintain high humidity, and kept at room temperature for 5 days. Before SECM measurements, the electrodes were rinsed with 20 mM tris-ClO_4 buffer and dried in a stream of argon. The M-DNA monolayer was prepared by exposing the ds-DNA monolayer to a solution of 0.3 mM $Zn(ClO_4)_2$ in 20 mM tris-ClO_4 buffer (pH 8.6) for at least 2 h.

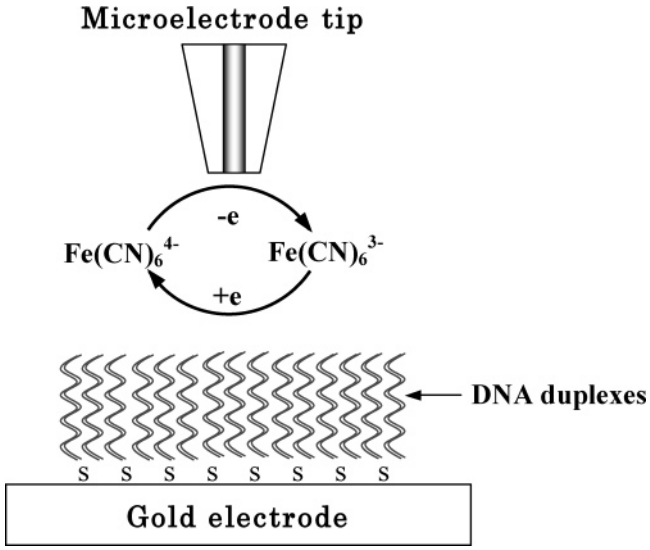

Figure 1. Schematic diagram of SECM measurement of electron transfer through DNA duplexes.

SECM Instrumentation and Procedure. Electrochemical experiments were carried out with a CHI-900 scanning electrochemical microscope (CH Instruments, Austin, TX) employing a three-electrode cell with the gold electrode as the working electrode, a platinum wire as the counter electrode, and Hg/Hg_2SO_4 (saturated with K_2SO_4) as the reference electrode. The SECM approach curves were obtained with a 25-μm-diameter Pt or Au tip. These tips were polished with 0.05-μm alumina before each experiment. The DNA-modified gold electrode was attached to the bottom of a Teflon cell using an O-ring. The solution was purged with argon for 10 min before measurements.

Results and Discussion

Electron Transfer at DNA Monolayers with Tip-Generated $Fe(CN)_6^{3-}$. SECM has recently been used to measure the rates of electron-transfer across self-assembled alkanethiol monolayers.[12] In the present work, we applied a similar strategy to measure the rate of ET through ds-DNA and M-DNA monolayers. In the feedback mode of SECM, a redox mediator, such as $Fe(CN)_6^{4-}$, is oxidized at the tip electrode with the tip potential adjusted to oxidize $Fe(CN)_6^{4-}$ at a diffusion-controlled rate. When the tip is far away from the DNA-modified gold substrate, a steady-state current, $i_{T,\infty}$, flows. This current results from the hemispherical diffusion of $Fe(CN)_6^{4-}$ to the tip. As the tip is brought close to the substrate, i.e., within a few tip radii, the $Fe(CN)_6^{3-}$ generated at the tip diffuses to the DNA/solution interface where it can be reduced via ET through the DNA monolayer (Figure 1). This process generates $Fe(CN)_6^{4-}$ at the interface and produces an enhancement in the faradic current at the tip electrode depending on the tip/substrate separation and the rate of ET through the DNA monolayer. Quantitative theory has been developed for different modes of

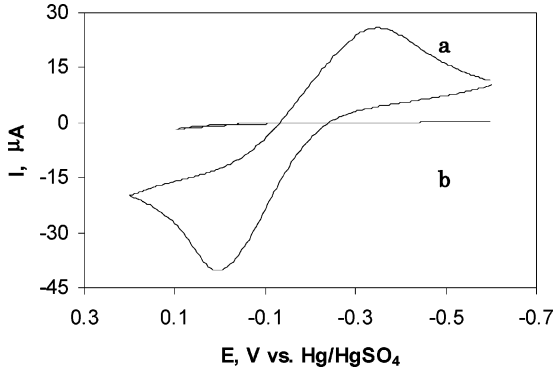

Figure 2. Cyclic voltammograms for 1 mM $K_4Fe(CN)_6$ in 20 mM Tris-ClO_4/50 mM $NaClO_4$ (pH 8.5) at a bare (a) and a ds-DNA-modified gold electrode (b). The potential scan rate was 100 mV/s.

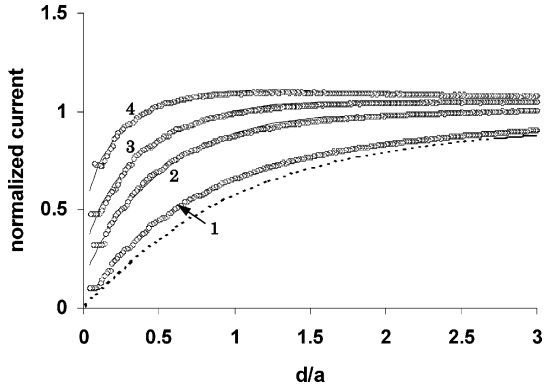

Figure 3. SECM approach curves obtained on a ds-DNA-modified gold electrode in a solution containing 1 mM $K_4Fe(CN)_6$, 50 mM $NaClO_4$, and 20 mM Tris-ClO_4 (pH 8.5). The tip was a 12.5-μm-radius Au disk. The tip potential was 0 V vs Hg/ Hg_2SO_4. The substrate potential was (1) −0.3, (2) −0.45, (3) −0.5, and (4) −0.6 V. The approaching speed was 1 μm/s. The solid lines are the SECM theoretical curves. The dashed line is the theoretical curve for pure negative feedback.

the SECM operation,[16] and the apparent rate constant of ET through the DNA monolayer can be extracted by fitting experimental tip current (i_T) versus distance (d) curves (called "approach curves") to the theory. Approach curves can also be obtained by reducing the mediator, for example, $Fe(CN)_6^{3-}$, at the tip and oxidizing the tip-generated species, $Fe(CN)_6^{4-}$, at the DNA substrate.

Figure 2 shows the cyclic voltammograms of $Fe(CN)_6^{4-}$ at a DNA-modified gold electrode. The lack of a redox signal at the modified electrode indicates that the gold electrode surface was covered by the ds-DNA monolayer with few defects. As reported previously,[17,18] penetration of the DNA monolayer by $Fe(CN)_6^{3-}$ has a low probability because of the electrostatic repulsion between the negatively charged phosphates on the DNA chains and the solution anions.

Figure 3 shows the SECM approach curves obtained on a ds-DNA-modified gold electrode using tip-generated $Fe(CN)_6^{3-}$ as the redox probe. When the overpotential of the substrate was small (e.g., $E_S = -0.3$ V vs Hg/Hg_2SO_4), the SECM feedback was so weak that the approach curve obtained at this potential was close to the theoretical curve for pure negative feedback over an insulator (the dashed line in Figure 3). A measurable feedback was observed as the substrate overpotential became more negative, indicating that the rate of the regeneration of $Fe(CN)_6^{4-}$ at the ds-DNA-modified gold was faster at a higher substrate overpotential. The ability of using SECM with large overpotentials is an important advantage over voltammetric

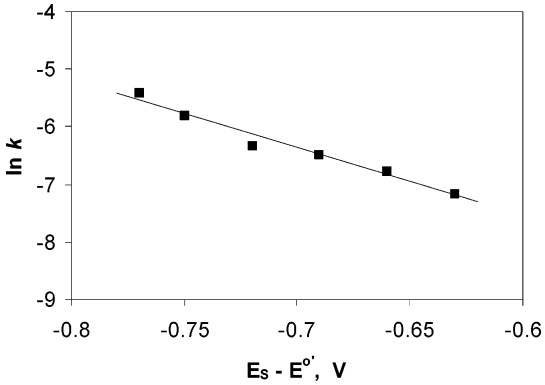

Figure 4. The apparent rate constant (k) vs substrate potential measured at a ds-DNA-modified gold electrode in a solution containing 1 mM $K_4Fe(CN)_6$, 50 mM $NaClO_4$, and 20 mM Tris-ClO_4 (pH 8.5). k was determined by fitting the approach curves as shown in Figure 3 to SECM theory.

TABLE 1: Standard Rate Constants for Electron Transfer between $Fe(CN)_6^{3-}$ and Gold Electrode through DNA and M-DNA Monolayers[a]

sample	k^0, (cm/s)
Au	$(2.5 \pm 0.1) \times 10^{-4}$
ds-DNA/Au	$(4.6 \pm 0.2) \times 10^{-7}$
M-DNA/Au	$(5.0 \pm 0.3) \times 10^{-6}$

[a] Deviations shown represent repeated measurements with three different monolayer samples.

approaches to heterogeneous kinetic measurements. Apparent rate constants of ET through the DNA monolayer can thus be obtained by fitting the approach curves to theory. Figure 4 shows the rate constants, k, vs substrate potential. The standard ET rate constant, k^o, was derived assuming the Butler−Volmer equation holds:

$$k = k^0 \exp[-\alpha F(E_S - E^{o\prime})/RT] \quad (1)$$

where α is the transfer coefficient, $E^{o\prime}$ is the formal potential of the redox probe, F is Faraday's constant, R is the gas constant, and T is the temperature. The value of k^o obtained from Figure 4 using eq 1 is listed in Table 1, along with the value of k^o for ET at a bare gold electrode measured following the same procedure.

The SECM feedback at a M-DNA-modified gold electrode is shown in Figure 5. The M-DNA monolayer was prepared by exposing the ds-DNA monolayer to a solution of 0.3 mM $Zn(ClO_4)_2$ in 20 mM tris-ClO_4 buffer (pH 8.6) for 2 h. For comparison, the SECM feedback at bare and native ds-DNA-modified electrodes is also shown in Figure 5. The SECM feedback at the M-DNA-modified electrode (curve 2) is much higher than at the native ds-DNA-modified electrode (curve 1). In previous studies, M-DNA was shown to convert readily back to B-DNA upon addition of EDTA, which chelates Zn^{2+}.[6] After the M-DNA-modified electrode was dipped into 20 mM tris-ClO_4 buffer (pH 8.6) containing 1 mM EDTA for 10 min, the SECM feedback decreased and the approach curve was almost identical to curve 1 (not shown in Figure 5). This result is in agreement with those obtained from voltammetric, chronocoulometric, and AC impedance measurements.[10,11] The voltammetric measurements for the $[Fe(CN)_6]^{3-/4-}$ probe at a M-DNA monolayer exhibited a significantly increased signal as compared to that of a ds-DNA monolayer. Upon adding EDTA to buffer containing M-DNA monolayer, the signal decreased significantly.[10] Following the same procedure used for measuring k^o

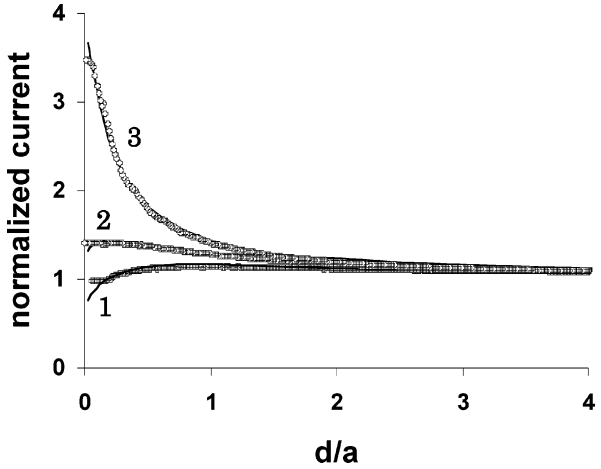

Figure 5. SECM approach curves obtained on a ds-DNA-modified gold electrode (1), a ds-DNA-modified gold electrode soaked in 0.3 mM $ZnClO_4$ for 2.5 h (2), and a bare gold electrode (3). The solution contained 1 mM $K_4Fe(CN)_6$, 50 mM $NaClO_4$, and 20 mM Tris-ClO_4 (pH 8.5). The tip was a 12.5-μm-radius Au disk. The tip and substrate potential were 0 and -0.65 V vs $Hg/HgSO_4$, respectively. The approaching speed was 1 μm/s. The solid lines are the SECM theoretical curves.

for ET at the ds-DNA-modified electrode, the value of k^o for ET at the M-DNA-modified electrode was obtained and is listed in Table 1, indicating that the ET rate at an M-DNA monolayer is about 1 order of magnitude higher than at a B-DNA monolayer.

The increased signal found at the M-DNA monolayer was ascribed to an increased ET rate from the redox probe through the DNA helix to the electrode surface.[10] Enhanced electron transport in M-DNA was also observed in recent fluorescent studies, which demonstrate effective quenching in a M-DNA duplex of a fluorescein donor by a rhodamine acceptor over 20 base pairs.[7] With B-DNA under the same conditions, quenching did not take place. Direct measurements of the conductive properties of M-DNA stretched between gold electrodes show it to have "metallic" conductive properties, whereas under these conditions B-DNA was said to be a semiconductor with a wide band gap.[19] The metal ions in the M-DNA could be involved in a stacking interaction of the base pairs and promote ET through DNA duplexes. However, a detailed mechanism for facilitated electron transport in M-DNA is still not clear.

Electron Transfer at DNA Monolayers with Tip-Generated $Fe(CN)_6^{4-}$. The above measurements were made with tip-generated $Fe(CN)_6^{3-}$ and probed electron transfer at the DNA-covered substrate. A similar approach can probe hole transfer (oxidation) at the substrate by generating $Fe(CN)_6^{4-}$ at the tip. Figure 6 shows the cyclic voltammogram of a DNA-modified gold electrode in 20 mM Tris-ClO_4 buffer (pH 8.5) containing 1 mM $K_3Fe(CN)_6$ and 50 mM $NaClO_4$. The solid line represents the CV curve obtained on a bare gold electrode in the same solution. The SECM feedback at the DNA-modified gold electrode is shown in Figure 7 (curve 1). The B-DNA was then converted into M-DNA by exposing the ds-DNA monolayer to a solution of 0.3 mM $Zn(ClO_4)_2$ in 20 mM tris-ClO_4 buffer (pH 8.5) for 2 h. Curve 2 in Figure 7 is the SECM approach curve obtained on the M-DNA monolayer. After curve 2 was recorded, the M-DNA was converted back into B-DNA by dipping it in the 20 mM tris-ClO_4 buffer (pH 8.5) containing 1 mM EDTA for 20 min. The approach curve was recorded again, as shown in Figure 7 (curve 3). Rate constants obtained by this procedure

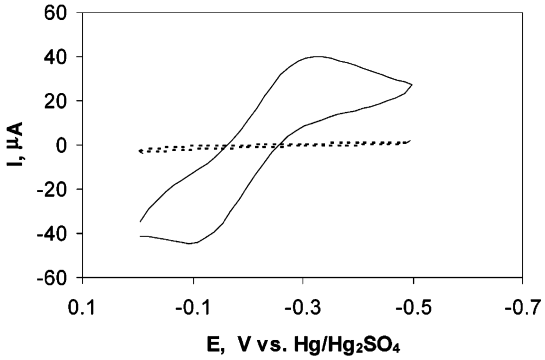

Figure 6. Cyclic voltammograms for 1 mM $K_3Fe(CN)_6$ in 20 mM Tris-ClO_4/50 mM $NaClO_4$ (pH 8.5) at a bare (solid line) and a ds-DNA-modified gold electrode (dashed line). The potential scan rate was 100 mV/s.

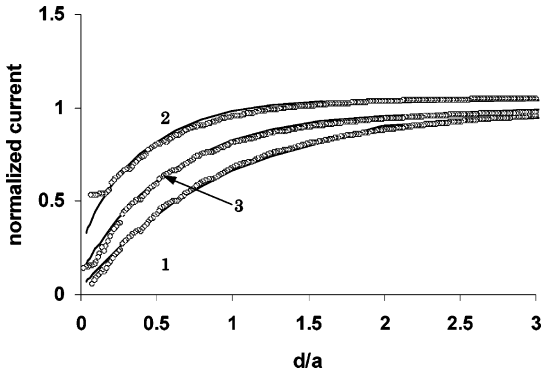

Figure 7. SECM approach curves obtained on a ds-DNA-modified gold electrode before (1) and after (2) the DNA monolayer was treated with Zn^{2+}. The electrode was then soaked in a Tris-buffer (pH 8.5) containing 1 mM EDTA for 20 min to remove the DNA-bound Zn^{2+} (3). The solution contained 1 mM $K_3Fe(CN)_6$, 50 mM $NaClO_4$, and 20 mM Tris-ClO_4 (pH 8.5). The tip was a 12.5-μm-radius Pt disk. The potentials of tip and substrate were -0.45 and 0.1 V vs $Hg/HgSO_4$, respectively. The approaching speed was 1 μm/s. The solid lines are the SECM theoretical curves. The rate constants (k) corresponding to these curves are (1) 0.00020, (2) 0.0015, and (3) 0.00064 cm/s.

TABLE 2: Standard Rate Constants for Electron Transfer between $Fe(CN)_6^{4-}$ and Gold Electrode through DNA and M-DNA Monolayers[a]

sample	k^0, (cm/s)
ds-DNA/Au	$(5.2 \pm 0.3) \times 10^{-7}$
M-DNA/Au	$(3.9 \pm 0.2) \times 10^{-6}$

[a] Deviations shown represent repeated measurements with three different monolayer samples.

are given in Table 2. The small difference between curves 1 and 3 might be caused by incomplete removal of Zn^{2+} or, more likely, some damage to the monolayer during the acquisition of the approach curves 1 and 2.

Electron Transfer at DNA Monolayers with Other Mediators. Although the SECM measurements appear to support the previous finding that electron transport via the M-DNA film is much faster than that by the native DNA film,[10] another ET pathway which can result in the enhancement of electron transport at the M-DNA-modified electrode has to be taken into account. The binding of metal cations to DNA reduces the negative charge of polyanionic phosphate backbones of DNA and hence reduces the electrostatic repulsion between the negatively charged phosphate backbone and the redox probe. The charge compensation of DNA backbones could facilitate approach of $Fe(CN)_6^{3-}$ to the underlying electrode surface and enhance the rate of electrode reaction of the redox mediator.

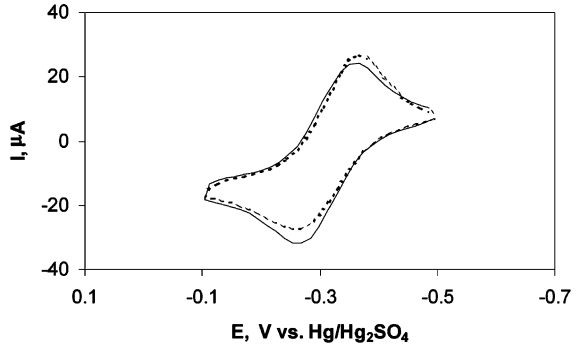

Figure 8. Cyclic voltammograms for 1 mM $Co(bpy)_3Cl_2$ in 5 mM Tris-HCl/50 mM NaCl (pH 7.1) at a bare (solid line) and a ds-DNA-modified gold electrode (dashed line). The potential scan rate was 100 mV/s.

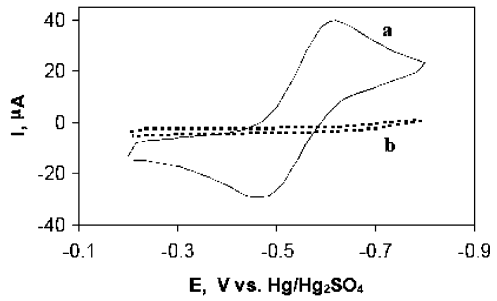

Figure 9. Cyclic voltammograms for 1 mM NaFe(III)EDTA in 20 mM Tris-HCl/50 mM NaCl (pH 8.5) at a bare (a) and a ds-DNA-modified gold electrode (b). The potential scan rate was 100 mV/s.

To test the effect of mediator charge on the blocking by DNA, similar experiments were carried out with neutral or positively charged mediators. Figure 8 shows the cyclic voltammograms at a ds-DNA-modified gold electrode and a bare gold electrode with the positively charged mediator $Co(bpy)_3^{2+}$ (bpy = 2,2′-bipyridyl) in solution which shows essentially no blocking by the DNA film. Other mediators such as ferrocenemethanol, ferrocenecarboxaldehyde, acetylferrocene, and $Ru(NH_3)_6^{3+}$ display similar voltammetric behavior, while $Co(phen)_3^{2+}$ (phen = 1,10-phenanthroline) penetrates although its voltammogram is somewhat perturbed from the bare-electrode one, perhaps because it can intercalate between DNA bases (results in Supporting Information). These results indicate that the redox reactions of these mediators at the DNA-modified electrode proceed virtually unimpeded, suggesting that these mediators can effectively penetrate the DNA monolayer.

Since uncharged and cationic mediators are not blocked by the DNA monolayer, we thought it of interest to test another anionic mediator. Figure 9 shows the cyclic voltammograms at a ds-DNA-modified gold electrode and a bare gold electrode with the negatively charged mediator, $Fe(III)EDTA^-$. The ET reaction of this mediator was significantly blocked by the DNA monolayer on gold surface, but was not blocked as effectively as $Fe(CN)_6^{3-}$ (compare Figures 2b and 9b). Presumably, the electrostatic repulsion between the negatively charged phosphate backbone and the mediator is larger for the −3 species $Fe(CN)_6^{3-}$ than for the −1 species $Fe(III)EDTA^-$. Note that ion pairing in solution, especially with $Fe(CN)_6^{3-}$, also occurs and will change the effective charge of the anions. Figure 10 shows the SECM approach curve obtained on a ds-DNA-modified gold electrode with $Fe(III)EDTA^{2-}$ as the tip-generated mediator species. After the DNA monolayer was treated with Zn^{2+} to form M-DNA, there was no change in the SECM feedback. These results suggest that electrostatic repulsion plays

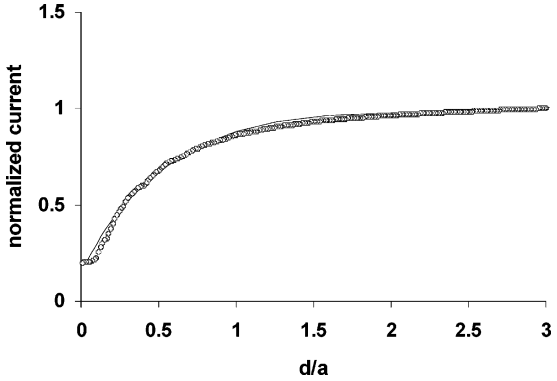

Figure 10. The SECM approach curve obtained on a ds-DNA-modified gold electrode in a solution containing 1 mM NaFe(III)EDTA, 50 mM NaCl, and 20 mM Tris-HCl (pH 8.5). The tip was a 12.5-mm-radius Au disk. The tip and substrate potentials were −0.7 and 0.1 V vs Hg/Hg_2SO_4 (saturated with K_2SO_4), respectively. The approaching speed was 1 μm/s. The solid line is the SECM theoretical curve.

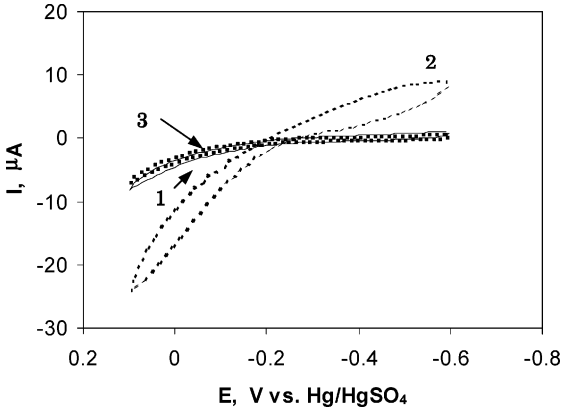

Figure 11. Cyclic voltammograms of 1 mM $K_4Fe(CN)_6$ in 20 mM Tris-ClO_4/50 mM $NaClO_4$ (pH 7) at a ds-DNA-modified gold electrode with the solution containing no Ca^{2+} (solid line) and 1 mM Ca^{2+} (dashed line, curve 1). After recording the CV curves in the solution containing Ca^{2+}, the DNA-modified electrode was dipped in the 20 mM tris-ClO_4 buffer (pH 7) containing 2 mM EDTA for 20 min and measured in the Ca^{2+}-free solution (dotted line). The potential scan rate was 100 mV/s.

a large role in the electrochemical behavior of mediator species and that differences in depth of penetration of the species in the monolayer, rather than electron transport through the DNA monolayer, could dominate the observed response. If this is the case, at least some of the effect of metal cations on the observed response can be attributed to their interaction with the phosphate groups on the backbone, decreasing the negative charge repelling the mediator.

There have been previous studies which indicated that the redox signal of $Fe(CN)_6^{3-/4-}$ on a DNA-modified electrode was significantly enhanced upon adding metal ions (e.g., Mg^{2+}, Ca^{2+}, and Ba^{2+}) or cationic intercalators, and the enhanced signal was ascribed to the charge compensation by the binding of the metal ions or cationic intercalators to DNA.[20−22] We carried out similar experiments with Ca^{2+} and Mg^{2+} as the binding metal ions. As shown in Figure 11, the voltammetric signal of $Fe(CN)_6^{3-/4-}$ on the ds-DNA-modified electrode was significantly increased upon adding 1 mM Ca^{2+} to the solution (dashed line). The electrode was then dipped in the 20 mM tris-ClO_4 buffer (pH 7) containing 2 mM EDTA for 20 min to remove Ca^{2+} bound to DNA. When the electrode was measured again in the solution containing no Ca^{2+}, the redox response of $Fe(CN)_6^{3-/4-}$ was restored (dotted line). Since Ca^{2+} is not complexed by the DNA

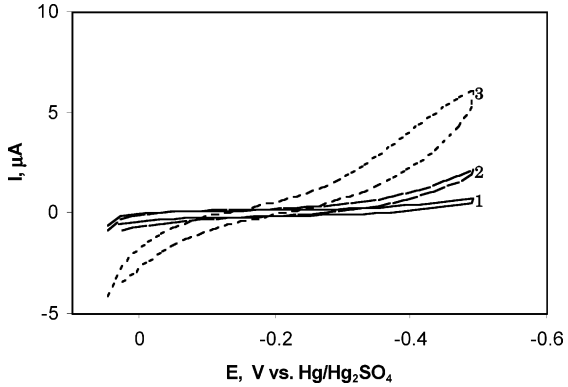

Figure 12. Cyclic voltammograms of 1 mM $K_3Fe(CN)_6$ in 20 mM Tris-ClO_4 (pH 8.5) containing (1) 0.05, (2) 0.2, and (3) 1 M $NaClO_4$ at a ds-DNA-modified gold electrode. The potential scan rate was 100 mV/s.

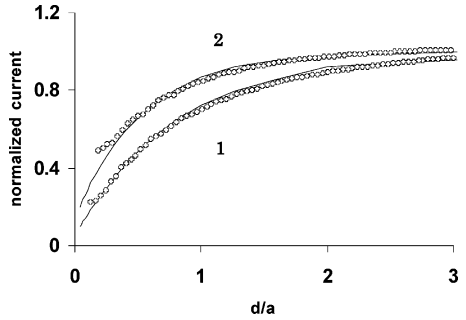

Figure 13. SECM approach curves obtained on a ds-DNA-modified gold electrode in 20 mM Tris-buffer (pH 8.5) containing 1 mM $K_3Fe(CN)_6$. The buffer contained (1) 50 mM and (2) 1 M $NaClO_4$. The tip was a 12.5-μm-radius Pt disk. The potentials of tip and substrate were -0.37 and 0.1 V vs $Hg/HgSO_4$, respectively. The approaching speed was 1 μm/s. The solid lines are the SECM theoretical curves. The rate constants (k) corresponding to these curves are (1) 3.5×10^{-4} and (2) 8.9×10^{-4} cm/s.

bases to form M-DNA[10] and only associates with the phosphate backbone, the enhancement of the redox signal shown in Figure 11 can probably be attributed to charge compensation of the DNA monolayer caused by the binding of Ca^{2+} to DNA phosphates. Similar results were obtained with Mg^{2+} as the binding metal ion.

The charge compensation effect was also investigated by measuring the redox response of $Fe(CN)_6^{3-/4-}$ on the ds-DNA-modified electrode at different concentrations of the supporting electrolyte in the buffer. As shown in Figure 12, the voltammetric signal of $Fe(CN)_6^{3-/4-}$ on the ds-DNA-modified electrode increased with the concentration of $NaClO_4$ in the buffer. SECM measurements gave similar results (Figure 13). The apparent ET rate constant increased from 3.5×10^{-4} to 8.9×10^{-4} cm/s when the concentration of $NaClO_4$ increased from 0.05 to 1 M. After the DNA monolayer was rinsed with a buffer containing no $NaClO_4$ and measured again in the buffer containing 0.05 M $NaClO_4$, the SECM response decreased and the approach curve was almost identical to curve 1 (not shown in Figure 13). These results further support the role of cation−DNA phosphate interactions facilitating monolayer penetration by $Fe(CN)_6^{3-/4-}$.

Conclusions

SECM was used to investigate electrochemical charge-transfer processes at a monolayer of DNA. Blocking of the electrochemical response was found only for anionic mediators, $Fe(CN)_6^{3-}$ and Fe(III)$EDTA^-$, suggesting that electrostatic repulsion between the mediator and the negatively charged phosphates on DNA and mediator penetration play a large role in the electrochemical response. The enhancement of the current with addition of Zn^{2+} occurred only with $Fe(CN)_6^{3-}$ and was also found with Ca^{2+} and Mg^{2+}, which do not coordinate with the DNA bases, suggesting that partial charge neutralization and facilitated penetration, rather than enhanced rate of electron-transfer across the self-assembled monolayer of DNA, were taking place. Although we cannot rule out some contribution from base stack-mediated ET to the increased ET rate at M-DNA monolayers, there are other problems with this route. If the transport occurs mainly by hopping of holes in oxidized bases or of electrons in reduced bases, the mediators used here and in most other studies do not have sufficiently large potentials to cause such oxidations and reductions of the bases. Moreover, the radical ions of the DNA bases are very unstable, so that hopping transport would have to compete with the decomposition of the radical ions. Thus, we suggest that the increased permeability of the redox probe in the M-DNA monolayers was the major contribution.

Acknowledgment. Support from the National Science Foundation (CHE 0109587) is greatly appreciated. This work was partially funded by NSERC. H.B.K. is the Canada Research Chair in Biomaterials.

Supporting Information Available: Cyclic voltammograms of some neutral or positively charged mediators at bare and ds-DNA-modified gold electrodes. This material is available free of charge via the Internet at http://pubs.acs.org.

References and Notes

(1) Lewis, F. D.; Letsinger, R. L.; Wasielewski, M. R. *Acc. Chem. Res.* **2001**, *34*, 159.

(2) Wagenknecht, H.-A. *Angew. Chem., Int. Ed.* **2003**, *42*, 2454.

(3) Schuster, G. B. *Acc. Chem. Res.* **2000**, *33*, 253.

(4) Delaney, S. D.; Barton, J. K. *J. Org. Chem.* **2003**, *68*, 6475.

(5) Long, Y. T.; Li, C. Z.; Sutherland, T. C.; Chahma, M.; Lee, J. S.; Kraatz, H. B. *J. Am. Chem. Soc.* **2003**, *125*, 8724.

(6) Lee, J. S.; Latimer, L. J. P.; Reid, R. S. *Biochem. Cell Biol.* **1993**, *71*, 162.

(7) Aich, P.; Labiuk, S. L.; Tari, L. W.; Delbaere, L. J. T.; Roesler, W. J.; Falk, K. J.; Steer, R. P.; Lee, J. S. *J. Mol. Biol.* **1999**, *294*, 477.

(8) Wettig, S. D.; Bare, G. A.; Skinner, R. J. S.; Lee, J. S. *Nanoletters* **2003**, *3*, 617.

(9) Aich, P.; Skinner, R. J. S.; Wettig, S. D.; Steer, R. P.; Lee, J. S. *J. Biomol. Struct. Dyn.* **2002**, *20*, 93.

(10) Li, C. Z.; Long, Y. T.; Kraatz, H. B.; Lee, J. S. *J. Phys. Chem. B* **2003**, *107*, 2291.

(11) Long, Y. T.; Li, C. Z.; Kraatz, H. B.; Lee, J. S. *Biophys. J.* **2003**, *84*, 3218.

(12) Liu, B.; Bard, A. J.; Mirkin, M. V.; Creager, S. E. *J. Am. Chem. Soc.* **2004**, *126*, 1485.

(13) Wincott, F.; Direnzo, A.; Shaffer, C.; Grimm, S.; Tricz, D.; Workman, C.; Sweedler, D.; Gonzalez, C.; Scaringe, S.; Usman, N. *Nucleic Acids Res.* **1995**, *25*, 2677.

(14) Delatorre, B. G.; Avino, A. M.; Escarceller, M.; Royo, M.; Albericio, F.; Eritja, R. *Nucleosides Nucleotides* **1993**, *12*, 993.

(15) Miller, C.; Cuendet, P.; Graetzel, M. *J. Phys. Chem. B* **1991**, *95*, 877.

(16) *Scanning Electrochemical Microscopy*; Bard, A. J., Mirkin, M. V., Eds.; Marcel Dekker: New York, 2001.

(17) Kelly, S. O.; Barton, J. K. *Bioconjugate Chem.* **1997**, *8*, 31.

(18) Yang, M.; Yau, H. C. M.; Chan, H. L. *Langmuir* **1998**, *14*, 6121.

(19) Rakitin, A.; Aich, P.; Papadopoulos, C.; Kobzar, Y.; Vedeneev, A. S.; Lee, J. S.; Xu, J. M. *Phys. Rev. Lett.* **2001**, *86*, 3670.

(20) Maeda, M.; Nakano, K.; Uchida, S.; Takagi, M. *Chem. Lett.* **1994**, *23*, 1805.

(21) Nakano, K.; Uchida, S.; Mitsuhashi, Y.; Fujita, Y.; Taira, H.; Maeda, M. *ACS Symp. Ser.* **1996**, *690*, 34.

(22) Park, N.; Hahn, J. H. *Anal. Chem.* **2004**, *76*, 900.